ISSN 1070-3632, Russian Journal of General Chemistry, 2014, Vol. 84, No. 10, pp. 1888–1892. © Pleiades Publishing, Ltd., 2014.
Original Russian Text © D.A. Vinnik, D.A. Zherebtsov, R. Niewa, L.I. Isaenko, G.G. Mikhailov, 2014, published in Zhurnal Obshchei Khimii, 2014, Vol. 84, No. 10, pp. 1607–1611.

Distribution of Dopant Metals between $PbTiO_3$ Crystals and $PbO–B_2O_3$ Flux

D. A. Vinnik[a], D. A. Zherebtsov[a], R. Niewa[b], L. I. Isaenko[c,d], and G. G. Mikhailov[a]

[a] *South Ural State University, pr. Lenina 76, Chelyabinsk, 454080 Russia*
e-mail: denisvinnik@gmail.com

[b] *Institute of Inorganic Chemistry, University of Stuttgart, Stuttgart, Germany*

[c] *Institute of Geology and Mineralogy, Siberian Branch, Russian Academy of Sciences, Novosibirsk, Russia*

[d] *Novosibirsk State University, Novosibirsk, Russia*

Received April 10, 2014

Abstract—Single crystals of lead titanate $PbTiO_3$ doped with silicon, calcium, chromium, manganese, cobalt, nickel, copper, zinc, and cadmium were grown. The compositions and crystallographic parameters of the crystals were studied. The lowest distribution coefficients of dopants between $PbTiO_3$ crystals and flux were observed with Mn^{+2} and Co^{+2} and the highest, with Ca^{+2}. Doping with niobium leads to the formation of solid solutions with the pyrochlore structure $A_2B_2O_7$ and even higher distribution coefficient. A correlation was found between dopant concentrations and crystal cell parameters.

Keywords: lead titanate, single crystals, lead oxide solid solutions

DOI: 10.1134/S107036321410003X

Lead titanate crystals have found application in frequency stabilizers, ultrasonic generators, and other instruments [1, 2]. Doping of $PbTiO_3$ opens wide possibilities for controlling its piezoelectric properties and endowing it with additional, for example, magnetic properties.

The first generation of $PbTiO_3$ offered advantages of high piezoelectric and electromechanical coupling coefficients. Doped piezoelectric single crystals $Pb(Mg_{1/3}Nb_{2/3})O_3–PbTiO_3$ (PMN–PT) and $Pb(Zn_{1/3}Nb_{2/3})O_3–PbTiO_3$ (PZN–PT) showed higher longitudinal piezoelectric and electromechanical coupling coefficients [3–6]. Such properties allowed production of higher throughput and more sensitive transducers compared with those on the basis of polycrystalline PZT ceramics.

Piezocrystals of the second generation showed high electromechanical characteriscits in wide range of temperatures, electric fields, and mechanical stresses, which made them less demanding in terms of temperature and applied displacement field. Crystals of the PIN–PMN–PT and PMN–PZT systems with higher ferroelectric phase transition point and coercive force are more promising candidates for instrument making applications [3].

The third generation single crystals are doped with a few metal cations for modifying electrochemical characteristics. Mn doped PT single crystals has greatly increased mechanical quality factors, which is quite important in such devices as transducers, ultrasound engines, or piezoelectric transformers [3].

Comparing the crystal generations with each other, we can note that the second generation crystals have twice as high Curie point and coercive force as those of the first generation crystals at comparable dielectric and piezoelectric characteristics. The mechanical quality factor of the third generation crystals is five time higher than the respective characteristic of the first generation crystals. These alterations are associated with a manganese-induced internal displacement [7–10].

This article presents data on the dopant distribution in the "crystal-solution" system with lead titanate grown by spontaneous crystallization from $PbO–B_2O_3$ flux.

Fig. 1. Crystals of lead titanate nyobate.

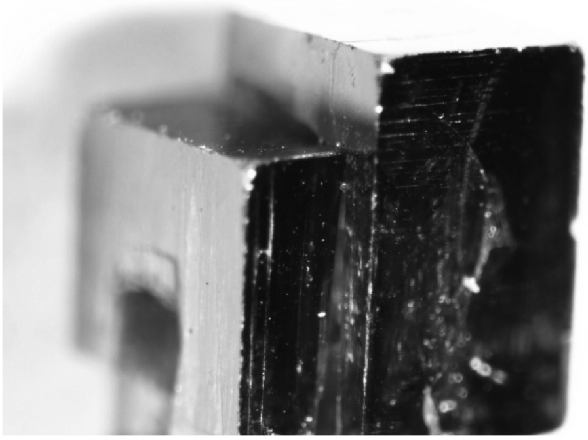

Fig. 2. Crystals of lead titanate doped with Cd ions.

EXPERIMENTAL

The optimal solvent for lead titanate at 900–1000°C is a mixture of lead and boron oxides [11]. The latter suppresses evaporation of PbO and thus ensures more stable crystallization of lead titanate in the solution.

As the starting components we used Ti(IV) oxide, Pb(II) oxide, boron oxide, and oxides of dopant components in a concentration of 5 mol % per Ti (Table 1). The total weight of the sample was 120 g.

Chemically pure grade reagents were used.

Single crystals were grown from solutions by spontaneous crystallization in air in a 40-mL platinum crucible placed into a resistance furnace. Temperature control was performed using a RIF-101 proportional, integral and derivative controller with a PR-30/6 thermocouple. All components of the mixture were preliminarily thoroughly ground in an agate mortar. The flux was heated at 1000°C for 2 h and then cooled to 925°C at a rate of 4 deg/h. The hot crucible was quickly taken from the furnace, and the rest of the flux was poured away (to measure its composition). The resulting crystals were separated from the solution residues by boiling in nitric acid.

The chemical composition of crystals and flux was determined by means of an Oxford INCA X-max 80 energy-dispersive X-ray fluorescence spectrometer mounted on a Jeol JSM-7001F scanning electron microscope. Parallel measurements were performed on no less than 5 crystals for each sample. X-ray phase analysis was performed on a DRON-3 diffractometer in the 2θ range 10°−80° at a scan rate of 1 deg/min.

The crystals of 2–5 mm we obtained at the experiment series. Mass of crystals in each experiment ranged from 12 to 18 grams. Color of crystals vary from pale yellow to dark yellow. All crystals, except doped with niobium, were of rectangular shape (Figs. 1, 2). Crystals containing niobium ions, has predominantly octahedral shape and a bright orange color.

Table 2 lists the concentrations of dopant cations in the flux at the beginning of the experiment (in the charge), as well as their concentrations in lead titanate and the flux. The scatter in dopant concentrations may be due to the difference in temperatures and solution compositions in the initial and final periods of crystal growth. Table 2 shows the minimal, maximal, and mean concentrations of dopant cations in crystals.

Table 1. Charge composition

Dopant oxide MO_x	Concentration, wt %			
	MO_x	PbO	TiO_2	B_2O_3
SiO_2	1.816	83.3	6.88	8.00
CaO	1.697	83.4	6.89	8.01
Cr_2O_3	4.469	81.06	6.69	7.78
MnO	2.137	83.00	6.86	7.97
MnO_2	2.606	82.64	6.82	7.93
CoO	2.254	82.82	6.84	7.95
NiO	2.247	82.94	6.85	7.96
CuO	2.390	82.82	6.84	7.95
ZnO	2.444	82.78	6.84	7.94
Nb_2O_5	7.563	78.43	6.48	7.53
CdO	3.802	81.63	6.74	7.83

Table 2. Dopant concentrations in the crystal and solution

Dopant	Concentration, wt %					Crystal–solution distribution coefficient
	charge	flux	crystal			
			minimum	maximum	medium	
Si	0.85	0.92	0.18	0.39	0.37	0.41
Ca	1.21	1.21	1.12	1.42	1.20	0.99
Cr	3.06	3.36	0.77	2.07	0.94	0.28
Mn^{+2}	1.65	1.85	0.17	0.25	0.23	0.12
Mn^{+4}	1.65	1.78	0.53	0.77	0.71	0.40
Co	1.77	1.99	0.16	0.31	0.23	0.12
Ni	1.76	1.80	0.58	1.84	1.50	0.83
Cu	1.91	2.12	0.28	0.65	0.42	0.20
Zn	1.96	2.18	0.25	0.65	0.40	0.18
Cd	3.33	3.74	0.32	0.55	0.49	0.13
Nb	5.29	2.91	17.79	24.16	21.92	7.53

Table 3. Unit cell parameters

Dopant	Concentraion in the crystal, mol %	*a*, Å	*c*, Å	*V*, Å^3	Ionic radius, Å
Si^{+2}	3.85	3.90117(19)	4.1538(4)	63.216(5)	0.40
Ca^{+2}	8.41	3.8928(3)	4.1489(5)	62.871(6)	1.00
Cr^{+3}	5.24	3.9043(6)	4.1291(6)	62.947(14)	0.615
Mn^{+2}	1.26	3.8998(3)	4.1317(6)	62.835(8)	0.67
Mn^{+4}	3.80	3.8990(3)	4.1260(8)	62.722(11)	0.53
Co^{+2}	1.17	3.9027(3)	4.1420(5)	63.286(7)	0.65
Ni^{+2}	7.29	3.9067(3)	4.1250(6)	62.958(7)	0.69
Cu^{+2}	1.97	3.9003(5)	4.1530(6)	63.177(8)	0.73
Zn^{+2}	1.83	3.9011(3)	4.1502(6)	63.159(7)	0.74
Cd^{+2}	1.31	3.9013(17)	4.1559(10)	63.254(16)	0.95
–	0.00	3.90096(18)	4.1546(24)	63.222(4)	–
–	0.00	3.89999(13)	4.1535(3)	63.174(4)	–
–	0.00	3.9015(4)	4.1535(5)	63.221(9)	–

Average dopant concentration was measured from a field with about 1000 crashed crystals. The crystal–solution distribution coefficient was determined as the ratio of dopant concentrations in the crystal and the charge.

It is interesting to note that the distribution coefficient of Ni is several times higher than those of Cr, Mn, Co, Cu, Zn, and Cd.

In the experiment with a niobium oxide dopant, the major phase is an oxygen-deficient pyrochlore $A_2B_2O_7$ phase with niobium in the solid solution: $Pb_2(Nb,Ti)_2O_{7-y}$ (Fig. 1). The substitution of titanium by niobium decreases the number of oxygen vacancies, thereby increasing the energy of the crystal lattice [12]. The X-ray analysis of the samples confirmed the tetragonal structure of the $PbTiO_3$. Among the dopant

metals studied just niobium has the highest crystal–flux distribution coefficient (Table 2). High distribution coefficients for the tetragonal solution were found for Ca and Ni in $PbTiO_3$. The reasons why nickel fairly easily enters the lead titanate lattice are likely to be associated with the possible partial existence of nickel in the trivalent state.

Table 3 lists the crystal lattice parameters for pure and doped samples, as well as the ionic radii of the corresponding cations (coordination number 6). The ionic radii of titanium and lead being substituted are 0.605 and 1.19 A, respectively [13].

The parameters of the crystal lattice of lead titanate are as follows: 3.902, 4.156 Å, and 63.278 $Å^3$ [14]. The average crystal lattice parameters of the nondoped crystals obtained in the present work are 3.901, 4.154 Å, and 63.206 $Å^3$, which is in a good agreement with the literature.

The solid solutions of dopants only slightly affect the crystallographic parameters of lead titanate (Table 3), which is due to the low dopant concentrations (per 1 mol of $PbTiO_3$). In the whole, the volume of the crystal lattice decreases with a decrease in the ionic radius of the dopant and an increase in its concentrations. The strongest effect is characteristic of the manganese cation which essentially decreases the unit cell volume. Calcium ions that substitute the larger Pb^{2+} ions in the lattice exert a similar effect and thus decrease the unit cell volume.

It is suggested that the other cations substitute the Ti^{4+} ion with the coordination number 4. Therewith, in most cases (except for Cd and Co) the unit cell volume decreases. One of the reasons of this effect is the formation of O^{2-} vacancies in order to maintain the charge balance. In Cd- and Co-doped crystals, the unit cell volume increases.

The doping with niobium results in the formation of a cubic structure like pyrochlore $A_2B_2O_7$, as reflected in octahedral crystal form (Fig. 2). The cell parameter is 10.4469(14) Å, which agrees with published data [12]. The crystal−flux distribution coefficient of Nb is 7.53±1.09, and this it is much larger than for the other dopants.

The crystal–flux distribution coefficients of dopants depend on the ratio of the bond energies in the crystal lattice of $PbTiO_3$ and in the lead−borate flux. When a cation is embedded into a crystal, its energy primarily depends on that, how much its radius and charge are close to the radius and charge of the cation to be substituted (Ti^{+4} or Pb^{+2}). In the lead−borate flux the most important factor is the basicity of the dopant, whereas the ionic radius is of secondary importance.

It should be noted that the valence of manganese (MnO and MnO_2 were introduced into the flux) much affects the crystal−flux distribution coefficients. This finding can be explained on the assumption that during experiment there is not enough time for the flux to equilibrate with air, and, consequently, Mn preserves the oxidation state characteristic of the starting oxide. Therefore, manganese added as MnO is present mostly as Mn^{2+}, whereas manganese introduced as MnO_2 remains in part as Mn^{4+}. Therewith, Mn^{4+}, which has a smaller radius, easier substitutes titanium cations. This is the reason for the much higher distribution coefficient in the case when manganese is introduced as MnO_2.

The fairly low content of relatively large cadmium ions in the crystal is likely to be associated with their stronger binding in the borate flux.

ACKNOWLEDGMENTS

The authors are grateful to D.M. Galimov, V.G. Zakharov, and O.S. Kolodkina (South Ural State University) for the help in research.

REFERENCES

1. Lv, H., Gao, H., Yang, Y., and Liu, L., *Appl. Catal. A*, 2011, vol. 404, p. 54. DOI: 10.1016/j.apcata.2011.07.010.
2. Chebanova, E.V., Kabiri, Y., Kupriyanov, M.F., Vasil, T.M., and Pustovaya, L.E., *Fazovyie perekhody, uporyadochennye sostoianya i novye materialy* (Phase Transitions Ordered States and New Materials), Rostov-on-Don: Rostov. Gos. Univ., 2007, vol. 7, p. 1.
3. Zhang, S. and Li, F., *J. Appl. Phys*., 2012, vol. 111, p. 031301. DOI: 10.1063/1.3679521.
4. Park, S.E. and Shrout, T.R., *J. Appl. Phys*., 1997, vol. 82, p. 1804. DOI: 10.1063/1.365983.
5. Fu, H. and Cohen, R.E., *Nature*, 2000, vol. 403, p. 281. DOI: 10.1038/35002022.
6. Davis, M., *J. Electroceram*., 2007, vol. 19, p. 23. DOI: 10.1007/s10832-007-9046-1.
7. Zhang, S.J., Lebrun, L., Randall, C.A., and Shrout, T.R., *J. Crystal Growth*, 2004, vol. 267, p. 204. DOI: 1016/

j.jcrysgro. 2004.03.063.

8. Priya, S., Kim, H.W., Ryu, J.H., Zhang, S.J., Shrout, T.R., and Uchino, K., *J. Appl. Phys*., 2002, vol. 92, p. 3923. DOI: 10.1063/1.1503411.
9. Zhang, S.J., Lee, M., Kim, D.H., Lee, H.Y., and Shrout, T.R., *Appl. Phys. Lett*., 2008, vol. 93, p. 122908. DOI: 10.1063/1.2992081.
10. Shrelock, N.P., Zhang, S.J., Luo, J., Lee, H.Y., Shrout, T.R., and Meyer, R.J., *J. Appl. Phys*., 2010, vol. 107, p. 074108. DOI: 10.1063/1.3359716.
11. Tamashpolsky, J.J., Venevtsev, Y., and Zhdanov, G.S., *Crystallography*, 1968, vol. 13, p. 521.
12. Bachelier, J., Hervieu, M., and Quemeneur, E., *Bull. Soc. Chim. Fr*., 1973, p. 2593.
13. Shannon, R.D., *Acta Crystallogr*., 1976, vol. 32, p. 751. DOI: 10.1107/S0567739476001551.
14. Nelmes, R.J. and Kuhs, W.F., *Solid State Commun*., 1985, vol. 54, p. 721. DOI: 10.1016/0038-1098(85) 90595-2.